Monthly Weather Review

VOLUME 98, NUMBER 9

SEPTEMBER 1970

UDC 551.521.14:551.507.362.2

A NEW STATISTICAL METHOD OF ESTIMATING SURFACE RADIANCES FROM CORRESPONDING SATELLITE WINDOW-CHANNEL RADIANCES

FRANK L. MARTIN [1] and VINCENT V. SALOMONSON

Goddard Space Flight Center, NASA, Greenbelt, Md.

ABSTRACT

Stepwise linear regressions for the specification of blackbody surface radiances are computed using a set of 103 model atmospheres chosen originally by Wark et al. and the corresponding simulated values of Nimbus 2 window-channel (10–11 μ) radiances. Two stratifications are considered: (a) precipitable water vapor, $u>1$, and (b) $u<1$ gm cm^{-2}. For each of five zenith angles considered, significant contributions are made in both regression formulas by inclusion of parameters representing the radiative transfer effects of water vapor and ozone. This regression formulation makes use of empirically derived expressions related to these effects over long atmospheric paths. The specification of the sample of surface radiances is in accordance with a multiple correlation coefficient exceeding 0.990 and 0.995 in the respective stratifications. Corrections for atmospheric effects to be applied to Nimbus 2 window-channel radiances in estimating the corresponding surface values are displayed in nomogramic as well as analytic forms.

1. INTRODUCTION

Martin and Tupaz (1968) devised gross parameters generally representative of the absorber masses of water vapor and carbon dioxide, as well as the surface temperature, to specify (with correlation coefficient 0.977) the total outgoing terrestrial flux from a sample of 63 model atmospheres drawn from the set of 106 such atmospheres listed in appendix A of Wark, Yamamoto, and Lienesch (1962*a*).[2] The Martin and Tupaz fluxes had been deduced from the total unfiltered radiances $I(\theta)$ computed by the radiative transfer theory of Wark et al. (1962*a*, 1962*b*) at each of the five zenith angles $\theta=0°$, 20°, 45°, 60°, and 78.5°. Application of a quadrature method of integration was then made in converting intensities at the top of the atmosphere into the hemispheric outgoing flux (equations 32 and 33 of Martin and Tupaz 1968). While the details of the WYL (1962*b*) radiative transfer theory will not be reviewed here, it suffices to note that the statistical form of the radiative transfer parameters used by Martin and Tupaz are in basic physical consistency with the WYL model.

In this paper, the authors have endeavored to make use of the filtered radiances, as simulated for the Nimbus 2 *window channel* (also called channel 2) and generated by WYL (1966) using the same radiational transfer theory to determine effective transmittances in terms of the previously mentioned *gross radiative transfer* parameters. In the current study, all of the 106 model atmospheres in appendix A of WYL (1962*a*) have been employed with three exceptions (atmospheres 11, 20, and 49) where the required surface humidities were not listed. Since the Nimbus 2 simulated radiances [3] $N_2(\theta)$ were computed at five different zenith angles, it is desirable for this study to introduce a slant-path ozone radiative transfer parameter to account for the wide variance of ozone absorber mass with zenith angle θ. In contrast, the ozone column-mass was not a significant predictor in the specification of total outgoing flux (Martin and Tupaz 1968) because there was little variance of ozone mass in that sample. As a final conclusion, the introduction of slant-path gross radiative parameters for each of the three gaseous constituents that interact with the radiative transfer in the channel 2 spectral region resulted in highly significant contributions to the statistical specifications of the surface channel 2 (blackbody) radiances hereafter denoted by $N_2(B)$. The parameterization of the radiative transfer variables adopted for the statistical treatment is discussed in section 2.

[1] This coauthor performed his contribution during his tenure as a National Academy of Sciences National Research Council Senior Postdoctoral Resident Research Associate with the National Aeronautics and Space Administration. He has since returned to the U.S. Naval Postgraduate School, Monterey, Calif.

[2] Henceforth, reference to all work of these authors will be abbreviated as WYL.

[3] Simulated radiances $N_2(\theta)$ based upon the effective response functions in channel 2 were kindly provided by WYL (1966). These response functions for channel 2 are found on page 50 of the *Nimbus II User's Guide* (Goddard Space Flight Center 1966).

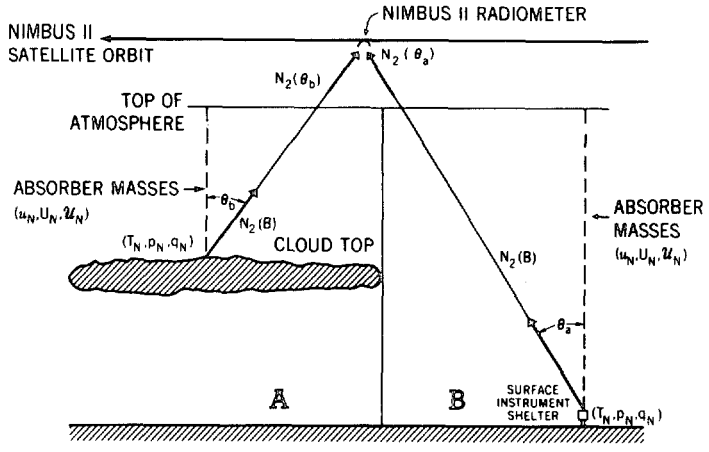

FIGURE 1.—Schematic depiction of the model-atmosphere types considered: (A) the cloud undercast situation and (B) the clear sky situation. The subscript N indicates the surface value of the indicated radiosonde parameters. The parameters, u_N, U_N, $\mathcal{U}_N$, represent the total absorber masses of water vapor, ozone, and carbon dioxide in the vertical, and (T_N, p_N, q_N) are the surface radiosonde parameters.

2. THE STATISTICAL MODEL

Of the 103 model atmospheres available in appendix A of WYL (1962*a*), cases 50–90 and 92–99 had an opaque cloud undercast that in each case was considered to be a blackbody surface accompanied by the cloud-top conditions of temperature (T_N), pressure (p_N), and mixing ratio (q_N). All of the other 54 cases from 1 through 106, with the exception of the three humidity rejections mentioned above, were clear-sky cases. The surface was again considered to be a blackbody associated with the surface-shelter conditions (T_N, p_N, q_N). A schematic depiction of the undercast and clear-sky conditions is given in figure 1.

The other parameters required for the statistical formulation are the total reduced absorber column masses in the vertical of water vapor, carbon dioxide, and ozone denoted by u_N, $\mathcal{U}_N$, and U_N, respectively. As in Martin and Tupaz (1968), the first two of these were simply pressure scaled (in accordance with the usual concept of pressure broadening of spectral lines) relative to their masses in the vertical. As a result, the *reduced* absorber masses of water vapor u_N and carbon dioxide $\mathcal{U}_N$ were designed in the forms

$$u_N = u_N P_{eN}^k$$

and

$$\mathcal{U}_N = 0.1\, p_N P_{eN}^k, \quad k = 0.85 \tag{1}$$

(Kuhn and Suomi 1965). Note that 0.1 p_N is an overestimate of the CO_2 absorber mass in terms of its generally quoted units of centimeters S.T.P. Its use is justified here purely on an empirical basis, that is, in the manner in which $\mathcal{U}_N$ is to be used for specification of $N_2(B)$, the coefficient 0.1 has been proved to give better results than alternative coefficients such as 0.05, 0.2, 0.4, etc.

The pressure-scaling factor involves the *effective* pressure P_{eN} from the top of the atmosphere (taken here to be $p=0.1$ mb) to $p=p_N$, defined after Cowling (1950) as

$$P_{eN} = \left(\int_0^{u_N} p\, du\right) \Big/ p_0 u_N. \tag{2}$$

In equation (2), u_N is the total precipitable water vapor where $u_N = g^{-1}\int_1^{p_N} q\, dp$. Typical values of the P_{eN}^k are listed in table 5 of Martin and Tupaz (1968) for a 63-case subsample of the total selection considered here.

Total ozone in centimeters S.T.P. was not pressure scaled because its interaction with the upwelling radiance, though systematic and statistically significant, is relatively small. Furthermore, the stepwise regression technique to be used essentially assigns a coefficient for the ozone contribution to the radiance (equation 3 below), and the coefficient may be viewed as a mean pressure-scaling effect in the context of the statistical model to be formulated.

As noted previously, the surface temperature T_N was taken to be that of a blackbody. From this point of view, the radiance $N_2(B)$ emitted from the surface was assumed to be related to that at zenith angle θ at the top of the atmosphere, $N_2(\theta)$, by an equation of the form

$$N_2(B) = A_1 + A_2 N_2(\theta) + A_3 X_3 + A_4 X_4 + A_5 X_5 \tag{3}$$

where X_3, X_4, X_5 (defined in equations 4 below) are the empirically selected functions of the slant-path absorber masses just discussed in connection with equations (1) and (2). The terms X_3, X_4, and X_5 simulate the interaction of the three constituents upon the upwelling radiance in channel 2 that emerges from the atmosphere to be recorded as $N_2(\theta)$ at the Nimbus 2 radiometer. For maintaining physical consistency with the model of WYL (1962*b*), the following conditions have been assumed: (a) flat earth, (b) horizontal homogeneity of all properties, and (c) no scattering effects.

The functions X_3, X_4, and X_5 of equation (3) were defined as

$$X_3 = N_2(B) \log (u_N \sec\theta), \tag{4a}$$

$$X_4 = N_2(B) \log (u_N \sec\theta) \log (U_N \sec\theta), \tag{4b}$$

and

$$X_5 = N_2(B) \log (u_N \sec\theta) \log (\mathcal{U}_N \sec\theta). \tag{4c}$$

Equations (4a), (4b), and (4c) introduce semiempirical representations of the gross radiative interactions by (a) water vapor alone, (b) the water vapor-ozone overlap, and (c) the water-vapor carbon-dioxide overlap. The rationale for formulating these functions (4a, 4b, and 4c) in this way lies in the fact that there exists both a weak water vapor band continuum and a group of weak lines of carbon dioxide within the channel 2 spectral region (Howard et al. 1956 and page 10 of Elsasser and Culbertson 1960). In addition, there is a well-defined strong band of ozone at 9.6 μ. According to a summary of these empirical

effects by Bandeen (1969), the water vapor continuum overlaps both of the other band intervals. However, relatively little is known regarding the exact overlap effects of the ozone and CO_2 lines in the spectral region of 9–12 μ that encompasses channel 2 of Nimbus 2 (page 50 of U.S. Goddard Space Flight Center 1966). Note that the slant-path absorber mass for each constituent has been related to the column-reduced mass by the multiplicative factor sec θ.

The use of logarithmic functions in X_3, X_4, and X_5 is consistent with the transmission curves of WYL (1962*a*, figs. 1, 4, and 5), especially for intermediate values of absorber mass. The use of logarithmic functions in equations (4) also tends to counteract the tendency of sec θ to increase too rapidly as θ increases, thus preserving a reasonable statistical model with regard to limb darkening.

The statistical modeling of $N_2(B)$ as formulated in equations (3) and (4) involves the generation of the nonlinear variables X_3, X_4, and X_5. All pertinent raw data such as T_N, p_N, P_{eN}, u_N, θ, U_N, $N_2(B)$, and $N_2(\theta)$ were encoded onto punched cards in consistent format. All of the other variables for input into equations (4) were developed internally to the regression procedure by transgeneration—a process that is an option of the stepwise regression program, BMD02R (Dixon 1966). The listing of $N_2(B)$ from initial values of T_N was accomplished by interpolation from table 1 that gives in detailed form the equivalence of blackbody temperature T_{BB} and channel 2 radiance in W/m²/sr (McCulloch 1969 and page 46 of Goddard Space Flight Center 1966).

TABLE 1.—*Relationship between equivalent blackbody temperature T_{BB} and the filtered radiance $N_2(B)$ in channel 2 (the window channel)*

Blackbody temperature, T_{BB} (° K)	Filtered radiance, $N_2(B)$ (W/m²/sr)	Blackbody temperature, T_{BB} (° K)	Filtered radiance, $N_2(B)$ (W/m²/sr)
170.0	0.361442	270.0	7.38773
180.0	.567252	280.0	8.88626
190.0	.849384	290.0	10.5564
200.0	1.22194	300.0	12.4008
210.0	1.69876	310.0	14.4208
220.0	2.29271	320.0	16.6164
230.0	3.01564	330.0	18.9884
240.0	3.87813	340.0	21.5352
250.0	4.88934	350.0	24.2552
260.0	6.05709	360.0	27.1463

3. THE STATISTICAL ANALYSIS

It was desirable to subdivide the total of 103 atmospheres investigated into two categories, $u_N < 1$ gm cm^{-2} and $u_N > 1$ gm cm^{-2}, because of relatively large differences of $N_2(B)$ across this value (table 2). Actually this criterion was relaxed somewhat because appendix A of WYL (1962*a*) gave listings for each case of total precipitable water vapor u_N. It was found that immediate separation of the cases into subdivisions could be effected by comparison of u_N with unity. The result of this simplified case stratification did not cause an appreciable loss in specification in the resulting multiple regression analysis.

SOME PRELIMINARY RESULTS OF THE SAMPLE STRATIFICATION

It is useful first to compare some of the statistics that emerge from the stratification into the two samples as just described. Table 2 illustrates some of the more important differences, particularly in the sample means and standard deviations of certain key variables that serve to describe the contrast in airmass properties. One such variable not previously defined is the effective transmittance, $\tau(\theta)$, defined here as

$$\tau(\theta)=N_2(\theta)/N_2(B). \tag{5}$$

The importance of the stratification is now evident. Sample 1 included 40 of the 49 overcast cases, most of which had relatively cool undercasts and small amounts of precipitable water vapor above the cloud. The nine clear-sky cases of sample 1 were typically cool polar continental airmasses. The requirement $u_N<1$ essentially separated the cool radiating surfaces from warm ones as evidenced by the differences in the sample means $\overline{N_2(B)}$. Another interesting difference relates to the mean transmittance $\bar{\tau}$ for the two stratifications averaged over all zenith angles. For the case $u_N<1$ gm cm^{-2}, the value $\bar{\tau}=0.8613$ resulted, whereas the more humid atmospheres are considerably less transparent ($\bar{\tau}=0.8124$).

RESULTS OF THE STEPWISE REGRESSION ANALYSIS

The procedure of developing stepwise regression equations in the form of equation (3), using the Miller screening technique (1962) to determine the order of entry of the four predictors $N_2(\theta)$, X_3, X_4, and X_5, is discussed next. This was actually done individually for the two stratifications. The screening technique as employed here first determines in an iterative manner the independent variable that explains the highest percent of the variance in $N_2(B)$; then at step 2, it determines that variable in the remaining predictor set that explains the largest percentage of the residual variance unexplained by the first variable, and so forth, on to the final predictor to be examined. The program also computed the F-statistic-upon-entry of the kth variable selected for the regression equation where F_k is expressible (at step k) as

$$F_k(1, n-k-1)=\left\{\frac{[\%\text{ cum. expl. var., step } k]-[\%\text{ cum. expl. var., step}(k-1)]}{[\%\text{ unexplained variance at step } k]}\right\}. \tag{6}$$

TABLE 2.—*Comparison of means and standard deviations* of some key variables*

	Stratification (1) $u_N<1$ gm cm^{-2}					Stratification (2) $u_N>1$ gm cm^{-2}				
	Sample 1, $n=66$ atmospheres					Sample 2, $n=37$ atmospheres				
Variable	$N_2(\theta)$	$N_2(B)$	$\tau(\theta)$	u_N gm cm^{-2}	U_N cm S.T.P.	$N_2(\theta)$	$N_2(B)$	$\tau(\theta)$	u_N gm cm^{-2}	U_N cm S.T.P.
	(W m^{-2} sr^{-1})					(W m^{-2} sr^{-1})				
Mean	5.0701	5.9264	0.86126	0.13033	0.30303	8.6455	10.6905	0.81241	1.3091	0.27484
Std. dev	1.3095	1.6405	0.03520	0.56007	0.05689	1.4997	1.9922	0.05382	0.22258	0.02783

*The standard deviation in the case of u_N and U_N is left in the logarithmic form $[\Sigma_i(\log u_{iN}/\bar{u}_N)^2/n]^{1/2}$ where n is the sample size.

In the present problem, there are four possible tests to be made using the four variables of the right side of equation (3) and a total possible sample size $n_1=330$ and $n_2=185$ in stratifications (1) and (2), respectively. Based upon the magnitudes of F_k, table 3 indicates the order of entry of the variables (predictors) selected and the corresponding values of F_k-upon-entry, after equation (6), henceforth symbolized as F_k.

For each predictor tested, its significance may be assessed at step k by comparison of its F_k value with a *critical* F at step k defined (after Miller 1962) as

$$F_c^k=F_{0.05/(P-k+1)}(1, n-k-1), \ \alpha=0.05. \tag{7}$$

Here, $k=1, 2, 3, 4$ is the step number, while $P=4$ is the number of possible predictors. The set of critical F_c^k values to be used for comparison takes on the values in table 4 (see also for example table 5 of Crow et al. 1960).

Since each of the F_k values of table 3 is considerably greater than the critical F_c^k value required for significance at the 95 percent confidence level (Miller 1962), the four-predictor multiple regression equations as printed out by the BMD02R program are

$$(u_N<1), \ N_2(B)=-0.02221+1.21397N_2(\theta)-0.07921X_3 -0.08055X_4+0.06988X_5 \tag{8a}$$

and

$$(u_N>1), \ N_2(B)=-1.02955+1.29395N_2(\theta)+0.55339X_3 +0.36390X_4-0.15662X_5 \tag{8b}$$

with multiple correlation coefficients of 0.9952 and 0.9902, respectively, and corresponding *standard errors* of estimate (S.E.) of 0.1616 and 0.2818 W m^{-2} sr^{-1}.

In the form of equations (8), $N_2(B)$ appears in the term for X_3, X_4, and X_5 on the right side. However, the regressions (8) had so little noise in the form of standard error that $N_2(B)$ and X_3, X_4, and X_5 will be treated as analytic functions. This device enables one to solve for $N_2(B)$ in the form of a function involving a numerator and denominator (see equations 13 below). It will be shown that use of $N_2(B)$ of equations (13) introduces very little additional unexplained variance than is given by equations (8).

TABLE 3.—*Stepwise order of entry of the predictors in the regression equation (3), including F_k-upon-entry at the indicated step. The multiple correlation R_k at each step is also included*

	Sample 1 ($n=300$), $u_N<1$ gm cm^{-2}			Sample 2 ($n=185$), $u_N>1$ gm cm^{-2}		
Step no.	Variable entered	F_k	Mult. correl. coeff., kth step	Variable entered	F_k	Mult. correl. coeff., kth step
$k=1$	$N_2(\theta)$	15635.0	0.9899	$N_2(\theta)$	1056.1	0.9232
2	$X_5(\theta)$	312.3	.9940	$X_5(\theta)$	676.0	.9842
3	$X_4(\theta)$	9.8	.9946	$X_4(\theta)$	78.5	.9890
4	$X_3(\theta)$	22.9	.9952	$X_3(\theta)$	21.2	.9902

Before leaving equations (8), it should be noted that the water vapor-carbon dioxide overlap term X_5 is highly dependent upon the other three variables of the right side. For arriving at specific results for X_5, the stepwise screening regression technique was again used leading to the relationships

$$(u_N<1), \ X_5=1.07374-0.25419 \ N_2(\theta)+2.0056 \ X_3 +0.12567X_4 \tag{9a}$$

and

$$(u_N>1), \ X_5= -0.62084+0.06392 \ N_2(\theta)+2.46622 \ X_3 +0.96111 \ X_4 \tag{9b}$$

with multiple correlation coefficients of 0.9667 and 0.9991 in the respective cases.

In arriving at the screened versions, equations (9a) and (9b), the discriminant technique of Miller (1962) based upon an analysis of the F_k-upon-entry was again employed. Each of the variables was accepted at a level far in excess of that required for 95 percent confidence estimate. The details are similar to those presented in connection with equations (6) and (7); therefore, they will not be repeated here.

It is of interest to note that X_5 given by equation (9b) had a multiple correlation coefficient of 0.9991. This suggests that any radiative transfer due to the weak band

TABLE 4.—*List of critical F values at step k*

		k=1	2	3	4	
F_c^k	Sample 1	6.5	5.9	5.1	3.9	$n_1=330$
	Sample 2	6.5	5.9	5.1	3.9	$n_2=185$

structure of CO_2 near 10 μ is masked by overlap effects associated with water vapor and ozone, especially in the stratification $u_N>1$. With $u_N<1$ gm cm^{-2}, the multiple correlation of 0.9667, while reasonably high, suggests that at least a measurable part of the simulated radiance $N_2(\theta)$ may be due to radiative transfer effects by the weak 10 μ lines of CO_2 that conceivably are not systematically accounted for in the water vapor continuum (page 10 of Elsasser and Culbertson 1960). This latter suggestion, however, has not been pursued further here.

At this point, the approximation of considering equations (9a) and (9b) to be analytic was repeated in connection with the similar approximation in regard to equations (8a) and (8b). By this device, X_5 was eliminated from each of (8a) and (8b) with the results

$$(u_N<1),\ N_2(B)=0.05282+1.19621\ N_2(\theta)+0.06094\ X_3 -0.00189X_4 \quad (10a)$$

and

$$(u_N>1),\ N_2(B)=-0.93231+1.28394\ N_2(\theta)+0.16713\ X_3 +0.21337X_4. \quad (10b)$$

The estimator $\hat{N}_2(B)$ formed by transgeneration from the variables of the right side of (10) when correlated with the actual values of $N_2(B)$ led to linear correlation coefficients of 0.9948 and 0.9896 in the respective cases and to corresponding standard errors of estimate of 0.1465 and 0.2875 W m^{-2} sr^{-1}.

4. ANALYTIC USE OF THE REGRESSION EQUATIONS

Because of the near equivalence of equations (8) and (10), the latter will be employed in the discussion that follows. Substitution for X_3 and X_4 from equations (4) followed by manipulation to bring all terms containing $N_2(B)$ to the left side leads to the results

$$\hat{N}_2(B)\ \{1-\log(u_N \sec\theta)\ [0.06094-0.00189\log(U_N \sec\theta)]\} =1.19621\ N_2(\theta)+0.05282 \quad (11a)$$

and

$$\hat{N}_2(B)\ \{1-\log(u_N \sec\theta)\ [0.16713+0.21337\log(U_N \sec\theta)]\} =1.28394\ N_2(\theta)-0.93231. \quad (11b)$$

The quasi-analytic forms, $\hat{N}_2(B)$, that serve as estimators of $N_2(B)$ are thus readily obtained from equations (11). Since (11) contain constants appropriate to the two stratifications dealt with here, it is convenient to introduce the sample means $\bar{u}$ and $\bar{U}$ whenever possible. Thus, we define

$$u_N=f\bar{u} \text{ and } U_N=F\bar{U} \quad (12)$$

where $\bar{u}$ and $\bar{U}$ have already been listed for both samples 1 and 2 in table 2. Combination of (11) and (12) together with the use of the sample-mean values for $\bar{u}$ and $\bar{U}$ leads to

$$\hat{N}_2(B)=\left\{\frac{1.13418N_2(\theta)+0.05001}{1-0.05871\log(f\sec\theta)-0.00158\log(F\sec\theta)+0.00179\log(f\sec\theta)\ \log(F\sec\theta)}\right\} \quad (13a)$$

and

$$\hat{N}(B)=\left\{\frac{1.29083N_2(\theta)-0.93732}{1-0.04595\log(f\sec\theta)-0.02509\log(F\sec\theta)-0.21452\log(f\sec\theta)\ \log(F\sec\theta)}\right\} \quad (13b)$$

for the cases $u_N<1$, $u_N>1$, respectively. The parameters f and F are the nondimensional measures in the vertical of the absorber masses of water vapor and ozone, respectively.

The estimator $\hat{N}_2(B)$ was computed from the right sides of equations (13) by transgeneration for each of the 330 data sets of case (a), and 185 data sets of case (b), and subjected to a linear regression analysis with the corresponding set of $N_2(B)$ values. The resulting linear regression analyses were

$$u_N<1,\ \hat{N}_2(B)=0.06639+0.98813\ N_2(B),$$
$$R(\hat{N}_2, N_2)=0.9943, \text{S.E.}=0.1471 \text{ W m}^{-2} \text{ sr}^{-1} \quad (14a)$$

and

$$u_N>1,\ \hat{N}_2(B)=0.27206+0.97473\ N_2(B),$$
$$R(\hat{N}_2, N_2)=0.9874, \text{S.E.}=0.3119 \text{ W m}^{-2} \text{ sr}^{-1} \quad (14b)$$

with $\bar{\hat{N}}_2(B)=5.9255$ and $\bar{\hat{N}}_2(B)=10.6925$ W m^{-2} sr^{-1} as the mean values of the predictands in the respective cases. These estimated means are to be compared with those given in table 2 for $\bar{N}_2(B)$ for samples 1 and 2, respectively. Note that $\hat{N}_2(B)$ turns out to be a very close estimate for $N_2(B)$ in either case.

Because of the small standard errors of estimate associated with equations (14), we have elected to use $\hat{N}_2(B)$ of (13) as our estimation formulas for use in the nomogram solution equivalent to equations (10) and/or (11).

5. A NOMOGRAM SOLUTION FOR SURFACE WINDOW RADIANCE $N_2(B)$

Equations (13) may be represented symbolically in the form $\hat{N}_2(B)=(\text{NUM})^*\ (\text{DENOM})^{-1}$. In turn, the reciprocal of the denominator varies between 1.3 and 0.98 when extreme values of f, F, and sec θ are introduced. Symbolically, (13) may be written as

$$\hat{N}_2(B)=(\text{NUM})^*\ (1\pm c) \tag{15}$$

where c is a positive number depending upon the parameters f, F, and θ (for samples 1 and 2). One also needs to know the choice of sign to introduce for any given set of these parameters.

Examples of the nomograms presenting c as a line-drawn system of curves involving f, F, and θ are shown in figures 2A and 2B. For the case $u_N<1$, c has the form

$$c=\left|\frac{0.05871\log(f\sec\theta)+0.00158\log(F\sec\theta)-0.00179\log(f\sec\theta)\log(F\sec\theta)}{1-0.05871\log(f\sec\theta)-0.00158\log(F\sec\theta)+0.00179\log(f\sec\theta)\log(F\sec\theta)}\right| \tag{16}$$

(see equation 13a) where vertical bars denote magnitude. Figure 2A illustrates the graph of log c, with c given by (16), for the special case log $F=0$, $u_N<1$, and for $f=4.0$, 2.0, 1.0, 0.5, 0.25, and for the full range of θ values extending from $\theta=0°$ to 85°. The results of the computation are presented here as the output of the CALCOMP plotter. Similarly for $u_N>1$ (fig. 2B) based upon (13b), the nomogram drawn for log c was computed from the equation

$$c=\left|\frac{0.04595\log(F\sec\theta)+0.02509\log(F\sec\theta)+0.21452\log(f\sec\theta)\log(F\sec\theta)}{1-0.04595\log(f\sec\theta)-0.02509\log(F\sec\theta)-0.21452\log(f\sec\theta)\log(F\sec\theta)}\right|. \tag{17}$$

The graphical results derived from equations (16) and (17) are not greatly different in appearance. Both have vertical cusps near $\theta=50°$ and $\theta=70°$, respectively. Any curve in figures 2A and 2B that sweeps from the lower left toward the upper right, regardless of the rate of change, is understood to be applicable in equation (15) with the *positive choice* of sign. The negative sign is applicable to those curves that sweep up from the lower right toward the upper left approaching the c axis.

Since for all practical purposes $c=10^{-5}$ is considered to be a negligible correction, the vertical cusps near $\theta=50°$ and $\theta=70°$ mark the boundary between a negative and a positive branch. On the c axis near $c\doteq10^{-2}$ and $c\doteq2\times10^{-2}$, there occur two horizontal-facing cusps (both associated with the conditions $\theta=0°$, log $F=0$). The value $c\doteq10^{-2}$ corresponds to the combination $f=2.0$ and $f=0.5$, whereas $c\doteq2\times10^{-2}$ is associated with the combination $f=4.0$ and $f=0.25$. Reciprocal f values in equations (16) and (17) give rise to identical c values at $\theta=0°$, but opposite signs are required in connection with their use in (15) that are determined by using the rules given in the preceding paragraph.

The interpretation of negative c for $f<1$ and of positive c for $f>1$ is that $\hat{N}_2(B)$ in the sample sets is consistently overestimated (underestimated) by the numerator alone in anomalously dry (moist) atmospheres and requires the multiplicative factors $(1-c)$ and $(1+c)$, respectively, for the appropriate radiance corresponding to the actual water vapor column paths. If the factor $(1\pm c)$ is simply reduced to 1, the correlation coefficient $R[\hat{N}_2(B), \text{NUM}]=0.9230$ instead of the value 0.9874 cited for $R[\hat{N}_2(B), N_2(B)]$ in equation (14b).

Additional nomograms that allow for variations in ozone have been examined (for example, log $F=0.06$, -0.06) but are not included here. These nomograms are only slightly different in appearance from those for log $F=0$ and can be generated quite easily by use of any of a number of commercially available digital line plotters.

From the solution (13), and the result (15), we see that

$$\hat{N}_2(B)=(\text{NUM})^*(1\pm c)=\text{constant}$$

depending upon T_N for each individual case. It is clear then that $N_2(\theta)$ experiences a limb-darkening effect given by

$$N_2(\theta)=\frac{\hat{N}_2(B)}{A_2}\left[1+c_w\log(f\sec\theta)+c_0\log(F\sec\theta)+c_{w0}\log(f\sec\theta)\log(F\sec\theta)\right]-\frac{A_1}{A_2} \tag{18}$$

where the constants c_w, c_0, c_{w0}, A_1, and A_2 are readily determined by examination of equations (13a) and (13b) for $u_N<1$ and $u_N>1$, respectively.

6. DISTRIBUTION OF ERRORS RESULTING FROM THE PREDICTION EQUATION

Making use of equations (13), the parameter ϵ defined as

$$\epsilon=\frac{\hat{N}_2(B)-N_2(B)}{N_2(B)} \tag{19}$$

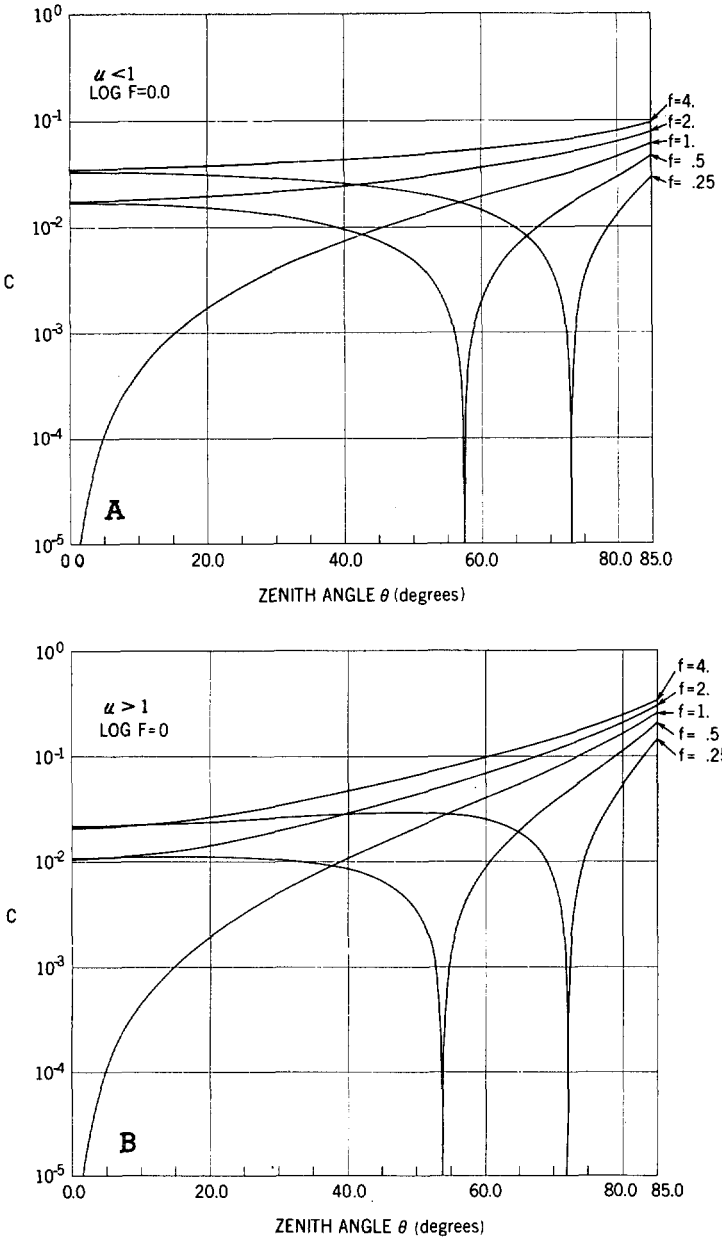

FIGURE 2.—(A) correction factor c on a logarithmic scale for determination of $N_2(B)$ from $N_2(B)=(1.13418N_2(\theta)+0.05001)^*(1\pm c)$, which is symbolic of equation (13a); curves or branches of curves that slope from lower left (right) toward upper right (left) assume the positive (negative) sign choice c; (B) is the same as (A), except that the product $(1\pm c)$ is used in connection with $N_2(B)=(1.29083N_2(\theta)-0.93732)^*(1\pm c)$, which is representative of equation (13b).

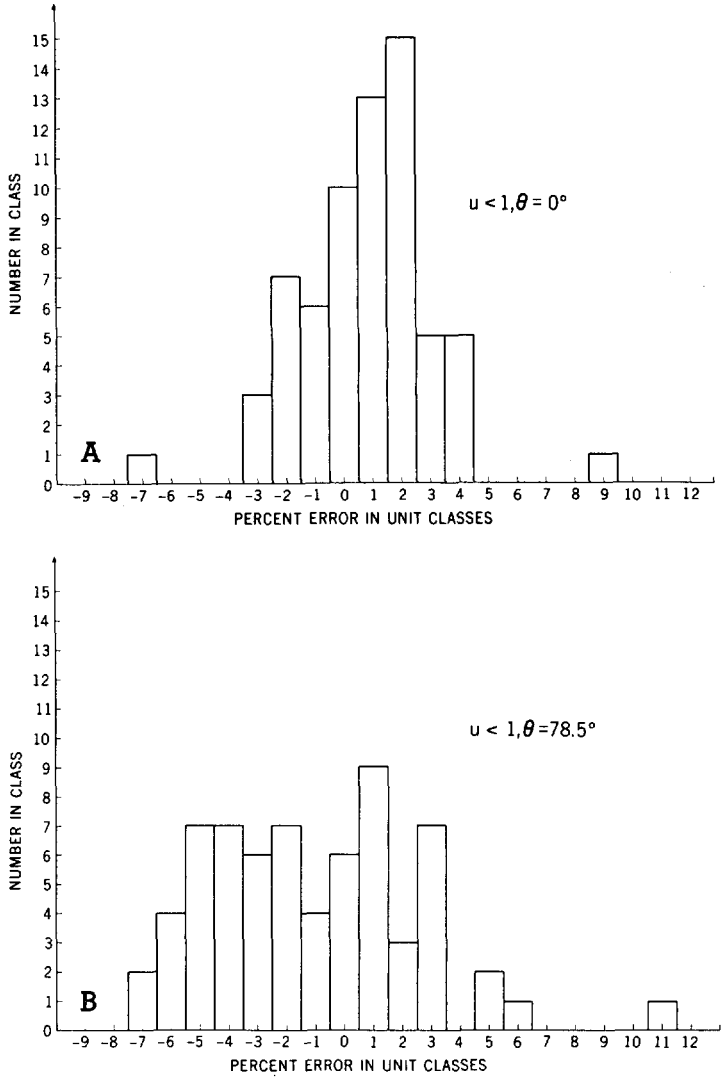

FIGURE 3.—Distribution of percentage errors resulting from the specification equation (13a) for $N_2(B)$, (A) for zenith angle $\theta=0°$ and (B) for $\theta=78.5°$.

was generated for each case. Here, ϵ represents the percent error of the predictions by (13a) and (13b). A histogram for $u_N<1$ is presented in figures 3A and 3B for the two zenith angles $\theta=0°$ and 78.5° and for $u_N>1$ in figures 4A and 4B for the same two angles. The total population in both parts of figure 3 is 66 while that of both figures 4A and 4B is 37. The mean in both figures 3A and 4A lies between 0.5 and 1 percent error; in both cases, the distribution is quite uniform about the mean error with only small variance.

In figures 3B and 4B, the mean error still remains in the same percent area as before (0.5 to 1 percent), but there is much greater variation in each case. There is a tendency for error classes to shift toward more extreme values in both the positive and negative senses as θ approaches 78.5°. Nevertheless, in both figures 3B and 4B ($\theta=78.5°$), approximately 75 percent of the cases lie within the error classes $|\epsilon|\leq 5$ percent.

7. CONCLUSIONS

When using a set of model atmospheres with flat earth symmetry, it has been shown that the effect of the major absorbers on radiances detectable by a satellite window channel can be accounted for by a statistical regression model. Verification using real atmospheres generally

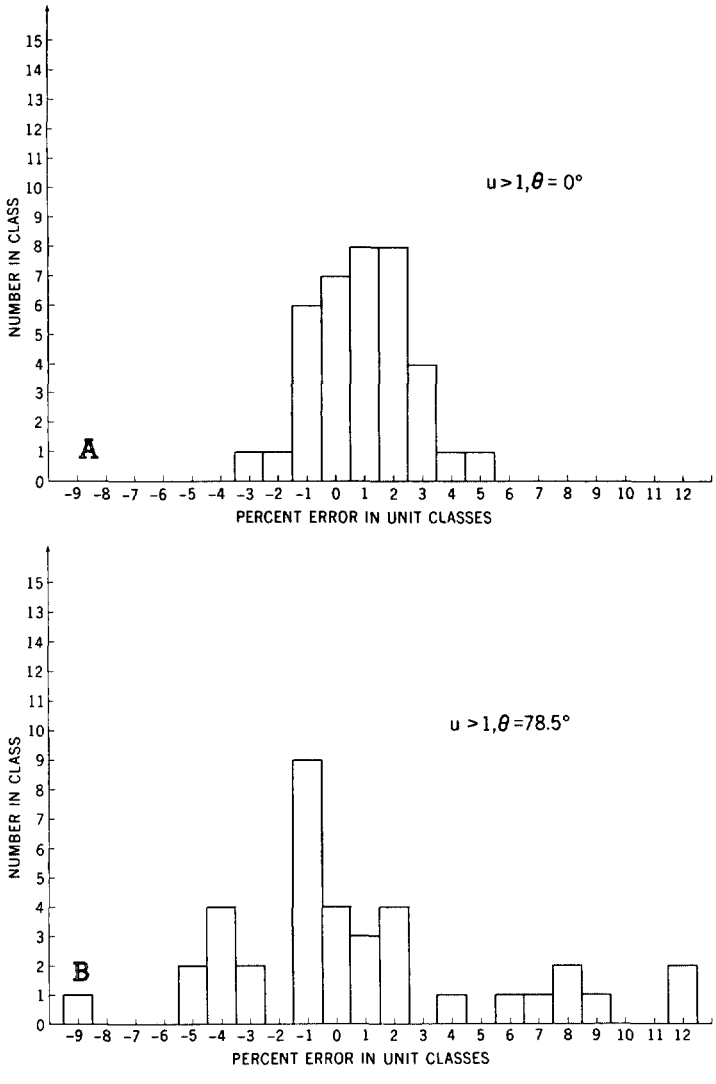

FIGURE 4.—Same as figure 3, except that equation (13b) is used for the determination of $N_2(B)$.

similar to those described in section 2 would have to be limited to small zenith angles because of the flat earth hypothesis and would be affected by the noise in specification of the mixing ratios of water vapor and ozone. In the radiative transfer computation of simulated radiances (WYL 1962*a*, 1962*b*) that led to our regression results, not only were all mixing ratios assumed exact but also subject to interpolation with a high degree of vertical resolution capability. This was necessary to give the exact measures of the absorber masses compatible with the application of radiative transfer theory. In verification using observed soundings, it is doubtful that the absorber masses could be specified with this degree of vertical resolution.

Nevertheless, it is felt that the statistical regression model presented here represents an approach to evaluating limb-darkening effects, particularly when dense, cold cloud layers are present. Further improvements along this line should be based upon radiative transfer computations in model atmospheres having spherical symmetry.

ACKNOWLEDGMENTS

The authors wish to thank Mr. William R. Bandeen for carefully reading and commenting on this paper. Appreciation is also expressed for the important programming assistance provided by Messrs. Hugh Powell and Dale Husk of Computer Applications, Inc.

REFERENCES

Bandeen, William R., "Experimental Approaches to Remote Atmosphere Probing in the Infrared From Satellites," *Atmospheric Exploration by Remote Probes, Final Report*, Vol. 2, National Academy of Sciences, National Research Council, Washington, D.C., Jan. **1969**, pp. 465–506.

Cowling, T. G., "Atmospheric Absorption of Heat Radiation by Water Vapour," *Philosophical Magazine*, Vol. 41, No. 313, Feb. **1950**, pp. 109–123.

Crow, E. L., Davis, F. A., and Maxfield, M. W., *Statistics Manual*, Dover Publications, Inc., New York, **1960**, 288 pp.

Dixon, W. J., *Biomedical Computer Programs*, Health Sciences Computing Facility, University of California, Los Angeles, **1966**, 585 pp.

Elsasser, Walter M., and Culbertson, Margaret F., "Atmospheric Radiation Tables," *Meteorological Monographs*, Vol. 4, No. 23, American Meteorological Society, Boston, Aug. **1960**, 43 pp.

Goddard Space Flight Center, *Nimbus II User's Guide*, National Aeronautics and Space Administration, Greenbelt, Md., July **1966**, 229 pp.

Howard, John N., Burch, Darrell E., and Williams, Dudley, "Infrared Transmission of Synthetic Atmospheres. I. Instrumentation," *Journal of the Optical Society of America*, Vol. 46, Nos. 3–6, Mar.–June **1956**, pp. 186–189, 237–241, 242–245, 334–338, and 452–455.

Kuhn, P. M., and Suomi, V. E., "Airborne Radiometer Measurements of Effects of Particulates on Terrestrial Flux," *Journal of Applied Meteorology*, Vol. 4, No. 2, Apr. **1965**, pp. 246–252.

Martin, F. L., and Tupaz, J. B., "A Numerical Procedure for Computation of Outgoing Terrestrial Flux Based Upon the Elsasser-Culbertson Model With Tests Applied to Model-Atmosphere Soundings," *Monthly Weather Review*, Vol. 96, No. 7, July **1968**, pp. 416–427.

McCulloch, A. W., U.S. Goddard Space Flight Center, National Aeronautics and Space Administration, Greenbelt, Md., **1969** (personal communication).

Miller, Robert G., "Statistical Prediction by Discriminant Analysis," *Meteorological Monographs*, Vol. 4, No. 25, American Meteorological Society, Boston, Oct. **1962**, 54 pp.

Wark, David Q., Yamamoto, G., and Lienesch, J. H., "Infrared Flux and Surface Temperature Determinations From TIROS Radiometer Measurements," *Report* No. 10, Meteorological Satellite Laboratory, U.S. Weather Bureau, Washington, D.C., Aug. **1962***a*, 84 pp.

Wark, David Q., Yamamoto, G., and Lienesch, J. H., "Methods of Estimating Infrared Flux and Surface Temperature From Meteorological Satellites," *Journal of the Atmospheric Sciences*, Vol. 19, No. 5, Sept. **1962***b*, pp. 369–384.

Wark, David Q., Yamamoto, G., and Lienesch, J. H., National Environmental Satellite Center, ESSA, Suitland, Md., **1966** (unpublished data).

[*Received September 29, 1969; revised April 29, 1970*]